



## Research paper

# Wave-based analytical solution for heat propagation in pavement structures

Mirosław Graczyk<sup>1</sup>, Józef Rafa<sup>2</sup>, Adam Zofka<sup>3</sup>, Leszek Rafalski<sup>4</sup>

**Abstract:** Pavements are layered systems from both the geometrical and physical points of view. Flexible pavements most often include a sequence of asphalt layers, typically composed of the wearing course, binder course and base course. So far, there is no definite analytical solution of such a layered system in relation to the temperature distribution that would consider different thermal properties of the respective layers and follow the physical laws of the thermal wave nature of heat propagation. This being so, we are unable to assess the effect of the thermal properties of the respective pavement courses on the overall temperature distribution in the asphalt portion. In multi-layer pavement systems also important are the phenomena taking place at the interfaces between the pavement courses which have a bearing on the service life of pavement. This article presents a new analytical solution to the problem of heat conduction and refraction in a multi-layer pavement. The solution was used to investigate and determine the effect of wave mode of heat propagation on the vertical temperature distribution, this considering that the pavement system is a sequence of layers comprising the soil subgrade, the base course and the wearing course. Moreover, the classical heat conduction equation is compared with the wave mode equation for a multi-layer pavement system and the temperature distribution in a layered system is compared with the temperature distribution in its homogenized equivalent. The solution of the heat conduction problem in a layered system showed a considerable effect of the thermal compatibility coefficients introduced by the authors and of the thermal refraction of the respective layers on the temperature distribution throughout the multi-layer pavement system. The output of this research includes prediction of the vertical temperature distribution in the pavement and definition of guidelines for reducing the effect of changing climatic conditions on the operation of layered flexible road and airfield pavements. In addition, the research results expand the toolkit for assessing the thermal effect on the actual pavements.

**Keywords:** multi-layer pavement, classical and thermal wave models of heat propagation, equivalent (homogenized) system, refraction coefficient, thermal compatibility

<sup>1</sup>PhD., Eng, Road and Bridge Research Institute, Instytutowa 1, 03-302 Warsaw, Poland, e-mail: [mgraczyk@ibdim.edu.pl](mailto:mgraczyk@ibdim.edu.pl), ORCID: 0000-0002-0601-7554

<sup>2</sup>Institute of Mathematics and Cryptology, Cybernetics Faculty, Military University of Technology, S. Kaliskiego 2, 00-908 Warsaw, Poland, e-mail: [jozef.rafa@wat.edu.pl](mailto:jozef.rafa@wat.edu.pl), ORCID: 0000-0001-8245-0109

<sup>3</sup>PhD., Eng, Road and Bridge Research Institute, Instytutowa 1, 03-302 Warsaw, Poland, e-mail: [azofka@ibdim.edu.pl](mailto:azofka@ibdim.edu.pl), ORCID: 0000-0002-6541-5966

<sup>4</sup>PhD., Eng, Road and Bridge Research Institute, Instytutowa 1, 03-302 Warsaw, Poland, e-mail: [lrafalski@ibdim.edu.pl](mailto:lrafalski@ibdim.edu.pl), ORCID: 0000-0002-6355-2596

## 1. Introduction

The models that have been used up to now for predicting the temperature distribution in pavements are based on the application of empirical or theoretical, for example FEM-based, relationships. Models of this kind are presented in a number of publications, including [1–9]. For example, in the Wistuba's method [10, 11] which is based on the numerical model governed by the Fourier's heat conduction equations the temperatures at different depths are obtained by iterative calculations of heat conduction between the ambient air, the pavement and the subgrade. The temperature values obtained in this way at a specific moment make up a so-called temperature profile.

The article by J. Górszczyk and W. Grzybowska [12] presents the results of a computer simulation of heat conduction governed by the Fourier equation in typical asphalt road pavements, including comparison to the actual temperature distributions in these pavements.

The articles of D. Wang [13, 14] present one- and two-dimensional axisymmetric analytical solutions for the temperature profile prediction in a multi-layer pavement system based on the classical heat conduction model, obtained using the trigonometric function series method.

In the article by Matthew R. Hall [15] the authors specify the effect of various thermophysical properties of the pavement material on the thermal behavior of the pavement systems in different U.S. climatic regions.

The report [16] presents models for the determination of summer and winter temperatures in asphalt pavements on the roads in Australia.

The MEPDG pavement design method uses the Enhanced Integrated Climatic Model EICM [17]. It is a one-dimensional forward finite-difference coupled heat and moisture flow model used to predict temperature and its seasonal variation over the pavement design life. This method provides numerical (quantitative) prediction of the vertical temperature distribution in the pavement. It does not, however, account for the qualitative effect of the relationship between the thermodynamic properties of the materials used for production of the respective pavement courses.

The approach used in [18] is based on the classical resolution of the Fourier's heat conduction equation.

The boundary conditions do not consider convective heat flux on the surface of the pavement under analysis. Moreover, the model does not apply to multi-layer pavement systems.

A classical one-dimensional heat conduction model is presented in [19] which considers a single layer only and ignores exchange of heat with the surroundings at the bottom interface of the layer (this being unreal adiabatic conditions). Numerical, finite difference method is used to obtain the solution.

The article [20] presents a numerical analysis of the transfer of heat generated by the cement hydration process during the initial setting of concrete in the pavement. The heat conduction equation describes the classical Fourier (i.e. non-wave) propagation of heat. The article provides a detailed analysis of the thermal phenomena taking place during

the hydration process. The results provide the guidance for the processes involved in the placement of concrete pavement.

Similar classical heat conduction problems of the layer/subgrade system are presented in [21] and [22].

Most publications on the subject present specific heat transfer solutions for single-layer systems which concern highly individualized issues and do not cover multi-layer pavement model, taking account of all the thermal actions involved, both external and internal, i.e. within the pavement system. It must be made clear that the existing publications do not provide a generalized analysis of the effect of general thermodynamic parameters of the pavement layer materials on the temperature distribution in the pavement and its thermal behavior resulting directly from the analytical solution. Introduction of dimensionless quantities referred to as thermal refraction coefficients enables a more in-depth analysis of the effect of the thermodynamic parameters on the temperature distribution in pavements. Moreover, this solution technique makes it possible to directly analyze factors such as the effect of the asphalt layers production process on minimizing the damaging thermal actions on the actual pavements.

The objective of this article is to present a new analytical solution to the problem of heat conduction and refraction in a multi-layer pavement system. The proposed solution is based on a description of the problem of heat conduction in a multi-layer system allowing for the external and internal heat exchange conditions and cyclic changes of temperature and heat flux. Before the new solution is presented in the following part of this article, the physical and mathematical assumptions of heat transfer modelling are defined. New heat propagation parameters have been introduced, namely: thermal impedance and the thermal wave reflection and refraction coefficients at the boundaries (interfaces) of the respective pavement courses. Two types of pavement, one designed for road the other for airfield paving, are used to present the effect of these parameters on the temperature distributions in the pavement courses.

## 2. Mathematical model of a three-layer pavement system – problem formulation

### 2.1. New analytical solution and verification of the pavement system homogenization

Let us consider a multi-layer pavement system, representing an actual road or airfield pavement. It is modelled by a typical sequence of asphalt layers or a PCC layer resting on a layered base system (Fig. 1).

The equation of the Gurtin-Pipkin model [23] governing wave propagation of heat in the  $i$ -th layer takes the following form:

$$(2.1) \quad \partial_t \left( \rho_i c v_i \theta_i(tz) + \int_0^t b_i(\tau) \theta_i(z, t - \tau) d\tau \right) - \partial_z^2 \int_0^t a_i(\tau) \theta_i(zt - \tau) d\tau = 0$$

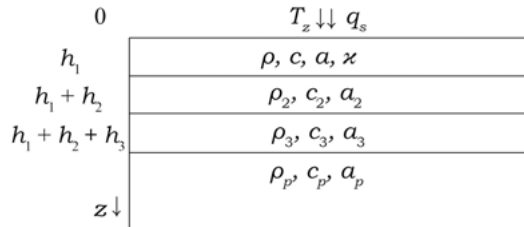


Fig. 1. Geometric model of pavement

where:  $\rho_i$ ,  $c_i$ ,  $a_i$  – density of the medium, specific heat and thermal conductivity in the respective pavement courses (in  $i$  layer) and in the subgrade;  $h_i$  – course thickness;  $\kappa$  – thermal conductivity at the top surface/air boundary (takes into account: windspeed, humidity, color);  $T_z$  – ambient temperature;  $q_s$  – ambient (solar) heat flux,  $bi$  – internal energy relaxation parameter,  $z$  – spatial variable,  $t$  – time,  $s$  – Laplace transform parameter,  $cv_i$  – specific heat (in  $i$  layer)

where now:

$$(2.2) \quad \theta_i = T_i - T_{0i} T_{0i} = T_i(0, z)$$

$T_i$  – absolute temperature in a layer,  $T_{0i}$  – initial temperature (constant in the respective layers) in the  $i$ -th layer.

The equation (2.1) models heat propagation by a thermal wave travelling at a speed.

$C_T$ , calculated as follows:

$$(2.3) \quad C_T = \sqrt{\frac{a(0)}{\rho Cv}}$$

Now let  $b(t) = 0$  and  $a(t) = k\delta(t)$  ( $\delta(t)$  – Dirac delta function) and then the equation (2.1) becomes a classical heat transfer equation with the speed of propagation tending to infinity.

Applying the Laplace transform to equation (2.1) with respect to time we obtain:

$$(2.4) \quad s(\rho_i cv_i + \bar{b}_i(s))\bar{\theta}_i(sz) - \bar{a}_i(s) \frac{d^2 \bar{\theta}_i(s, z)}{dz^2} = 0$$

where:

$$\bar{\theta}_i(sz) = L[\theta_i(tz)] = \int_0^{\infty} \theta_i(t, z) e^{-st} dt$$

$\bar{\theta}_i$ ,  $\bar{b}_i(s)$ ,  $\bar{a}_i(s)$  – Laplace transforms with respect to temperature and relaxation function  $i = 1, 2, 3, p$ .

Moreover, appropriate solutions of equation (2.4) satisfy the following boundary conditions subject to:

$$\begin{aligned}
 (2.5) \quad & z = 0 \\
 & -\bar{a}_1(s) \frac{d\bar{\theta}_1(s, 0)}{dz} + \kappa \bar{\theta}_1(s, 0) = \bar{q}_z(s) = \bar{q}_s + \kappa \bar{T}_z \\
 & z = h_1 \\
 & -\bar{a}_1(s) \frac{d\bar{\theta}_1}{dz} = -\bar{a}_2(s) \frac{d\bar{\theta}_2}{dz} \\
 & \bar{\theta}_1 = \bar{\theta}_2 \\
 & z = h_1 + h_2 \\
 & -\bar{a}_2(s) \frac{d\bar{\theta}_2}{dz} = -\bar{a}_3(s) \frac{d\bar{\theta}_3}{dz} \\
 & \bar{\theta}_2 = \bar{\theta}_3 \\
 & z = h_1 + h_2 + h_3 \\
 & -\bar{a}_3(s) \frac{d\bar{\theta}_3}{dz} = -\bar{a}_p(s) \frac{d\bar{\theta}_p}{dz} \\
 & \bar{\theta}_3 = \bar{\theta}_p
 \end{aligned}$$

The boundary conditions (2.5) express the equality of heat flux and temperature values at the boundaries between the pavement courses.

### 3. Solution of the problem of thermal actions in a three-layer pavement system

This yields the following equations being the solution of the formulated boundary problem (3.1)–(3.5) governing the wave propagation of heat in the respective pavement courses:

(3.1)

- in the first layer:  $0 < z < h_1$

$$\begin{aligned}
 \bar{\theta}_1(z, s) = & \frac{\bar{q}_z (1 + w_N)}{2i_1 M_3} \left[ (1 + w_{23}w_{3p}e^{-2h_3\gamma_3} + w_{12}w_{23}e^{-2h_2\gamma_2} \right. \\
 & + w_{12}w_{3p}e^{-2h_2\gamma_2}e^{-2h_3\gamma_3})e^{-z\gamma_1} \\
 & \left. + (w_{12} + w_{12}w_{23}w_{3p}e^{-2h_3\gamma_3} + w_{23}e^{-2h_2\gamma_2} + w_{3p}e^{-2h_3\gamma_3}e^{-2h_2\gamma_2})e^{-(2h_1-z)\gamma_1} \right]
 \end{aligned}$$

- in the second layer:  $h_1 < z < h_1 + h_2$

$$\begin{aligned}
 \bar{\theta}_2(z, s) = & \frac{\bar{q}_z (1 + w_N) (1 + w_{12})}{2i_1 M_3} \left[ (1 + w_{23}w_{3p}e^{-2h_3\gamma_3})e^{-(z-h_1)\gamma_2} \right. \\
 & \left. + (w_{23} + w_{3p}e^{-2h_3\gamma_3})e^{-(2h_2+h_1-z)\gamma_2} \right] e^{-h_1\gamma_1}
 \end{aligned}$$

- in the third layer:  $h_1 + h_2 < z < h_1 + h_2 + h_3$

$$\bar{\theta}_3(z, s) = \frac{\bar{q}_z}{2i_1} \frac{(1 + w_N)(1 + w_{12})(1 + w_{23})}{M_3} \left[ e^{-(z-h_1-h_2)\gamma_3} + w_{3p} e^{-(2h_3+h_1+h_2-z)} \right] e^{-h_1\gamma_1} e^{-h_2\gamma_2}$$

- and in the subgrade:  $z > h_1 + h_2 + h_3$

$$\bar{\theta}_p(z, s) = \frac{\bar{q}_z}{2i_1} \frac{(1 + w_N)(1 + w_{12})(1 + w_{23})(1 + w_{3p})}{M_3} \cdot e^{-(z-h_1-h_2-h_3)\gamma_p} e^{-h_1\gamma_1} e^{-h_2\gamma_2} e^{-h_3\gamma_3}$$

where:

$$(3.2) \quad \gamma_i = \sqrt{\frac{s(\rho_i c v_i + \bar{b}_i(s))}{\bar{a}_i(s)}} \quad \operatorname{Re} \gamma_i > 0 \quad r_{k,k+1} = \frac{\bar{a}_{k+1} \gamma_{k+1}}{\bar{a}_k \gamma_k}$$

is the coefficient of reflection (transmission) at the boundary between layers  $(k+1)$  and  $(k)$ :

$$(3.3) \quad \bar{a}_k \gamma_k = i_k$$

is the impedance (resistance) of  $k$ -th layer:

$$(3.4) \quad w_N = \frac{1 - r_N}{1 + r_N} \quad r_N = \frac{\kappa}{\bar{a}_1 \gamma_1} = \frac{\kappa}{i_1}$$

is the coefficient expressing the ratio between the Newton's and Fourier's heat fluxes (which can be interpreted as the reflection coefficient at the air/top layer interface):

$$(3.5) \quad w_{12} = \frac{1 - r_{12}}{1 + r_{12}} \quad w_{23} = \frac{1 - r_{23}}{1 + r_{23}} \quad w_{3p} = \frac{1 - r_{3p}}{1 + r_{3p}}$$

are the refraction coefficients at the boundaries between the pavement courses. They can, in theory, assume any value in the range of  $-1$  to  $1$ . In practice, however, this range is narrowed down to between  $-0.5$  and  $0.5$ .

Furthermore:

$$(3.6) \quad M_3 = 1 - w_N w_{12} e^{-2h_1\gamma_1} + w_{12} w_{23} e^{-2h_2\gamma_2} + w_{23} w_{3p} e^{-2h_3\gamma_3} + w_{12} w_{3p} e^{-2h_3\gamma_3} e^{-2h_2\gamma_2} - w_N w_{23} w_{3p} e^{-2h_3\gamma_3} e^{-2h_1\gamma_1} - w_N w_{23} e^{-2h_2\gamma_2} e^{-2h_1\gamma_1} - w_N w_{3p} e^{-2h_3\gamma_3} e^{-2h_2\gamma_2} e^{-2h_1\gamma_1}$$

### 3.1. Solution of homogenized pavement problem

Now let us replace the layered system presented in Fig. 1 with an equivalent homogenized layer resting on the same subgrade (Fig. 2), in accordance with the criteria presented

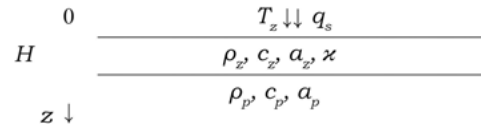


Fig. 2. Geometric model of a homogenized pavement

in detail in [24]. These criteria concerned, in particular, the equivalence of mass, equivalence of internal energy, equivalence of the temperature differential between the top (outer) surface and the subgrade, equivalence of parameters describing the wave propagation of heat in a multi-layer pavement system and its homogenized equivalent.

In the homogenized system (Fig. 2)  $H$ ,  $\rho_z$ ,  $c_z$ ,  $\kappa_z$  are the equivalent values of thickness, density of the medium, specific heat and thermal conductivity.

Considering equations (3.7) one obtains the following solution of the above problem: in the layer:  $0 \leq z \leq H$

$$(3.7) \quad \bar{\theta}(z, s) = \frac{\bar{q}_z(1 + w_N)}{2iM} \left[ e^{-z\gamma} + w e^{-(2H-z)\gamma} \right]$$

in the subgrade:  $z \geq H$

$$(3.8) \quad \bar{\theta}_p(z, s) = \frac{\bar{q}_z(1 + w_N)(1 + w)}{2iM} e^{-H\gamma} e^{-(z-H)\gamma_p}$$

where now:

$$(3.9) \quad \begin{aligned} r &= \frac{\gamma_p a_p}{\gamma a_z} = \frac{i_p}{i} & w_N &= \frac{1 - r_N}{1 + r_N} & r_N &= \frac{\kappa}{\gamma a_z} = \frac{i_0}{i} & i_0 &= \kappa \\ w &= \frac{1 - r}{1 + r} & i &= \gamma a_z \\ \gamma &= \sqrt{\frac{s(\rho_z c_z)}{a_z}} & \gamma_p &= \sqrt{\frac{s(\rho_p c_p)}{a_p}} \\ M &= 1 - w_N w e^{-2H\gamma} \end{aligned}$$

#### 4. The effect of the thermal compatibility between the courses on the behaviour of pavement

An important aspect of the analysis of heat conduction in multi-layer road and airfield pavements is to assess the effect of the thermal properties of the respective courses on refraction of waves at the respective interfaces including the road base/ subgrade interface. The numerical calculations, based on the new analytical solution, indicate a possibility to obtain good thermal compatibility of the pavement courses by adjusting the thermal parameters of the materials used for production of the respective asphalt layers. With appropriately selected impedances it is possible to influence the temperature distribution

and thermal stresses in the pavement, minimizing the undesired effects of factors such as thermal actions on the durability and strength of pavement. A significant element of this solution is refraction of thermal waves. It is described by two parameters:

$$r_{k,k+1} = \frac{\bar{a}_{k+1}\gamma_{k+1}}{\bar{a}_k\gamma_k}$$

which is refraction (transmission) coefficient at the boundary of layers ( $k+1$ ) and ( $k$ ), and  $w_N = \frac{1-r_N}{1+r_N}$ ,  $r_N = \frac{\kappa}{a_z\gamma}$ .

The above parameters define the degree of thermal compatibility between the respective pavement courses and the soil subgrade.

Full impedance matching considerably simplifies the processes of wave propagation and interaction in a layered system.

Wave refraction plays a significant role in the actual layered structures, such as road and airfield pavements. By appropriately selecting the thermomechanical parameters of the pavement courses and of the subgrade it is possible to minimize the damaging effects of the vehicle traffic and climatic factors on multi-layer pavements.

In order to illustrate the effect of the impedance matching on the temperature distribution in pavement let us assume there is a match between layers 1 and 2 and between layer 3 and the subgrade.

Thus, substituting  $w_{12} = 0$  and  $w_{3p} = 0$  yields:

$$\begin{aligned}
 \bar{\theta}_1 &= \frac{\bar{q}_z (1 + w_N)}{2i_1 \widetilde{M}_3} \left( e^{-z\gamma_1} + w_{23} e^{-2h_2\gamma_2} e^{-(2h_1-z)\gamma_1} \right) \\
 \bar{\theta}_2 &= \frac{\bar{q}_z (1 + w_N)}{2i_1 \widetilde{M}_3} \left( e^{-(z-h_1)\gamma_2} + w_{23} e^{-h_1\gamma_1} e^{-(2h_2+h_1-z)\gamma_2} \right) \\
 \bar{\theta}_3 &= \frac{\bar{q}_z (1 + w_N) (1 + w_{23})}{2i_1 \widetilde{M}_3} e^{-h_1\gamma_1} e^{-h_2\gamma_2} e^{-(z-h_1-h_2)\gamma_3} \\
 \bar{\theta}_p &= \frac{\bar{q}_z (1 + w_N) (1 + w_{23})}{2i_1 \widetilde{M}_3} e^{-h_1\gamma_1} e^{-h_2\gamma_2} e^{-h_3\gamma_3} e^{-(z-h_1-h_2-h_3)\gamma_p}
 \end{aligned}
 \tag{4.1}$$

where now:  $\widetilde{M}_3 = 1 - w_N w_{23} e^{-2h_2\gamma_2} e^{-2h_1\gamma_1}$ ,  $\bar{q}_z(s) = q_{z0}\bar{q}(s)$  and  $q_{z0} = q_{z0} + \kappa T_A$ ,  $q_0$  – solar flux amplitude,  $T_A$  – amplitude of the top surface/ambient air temperature differential,  $\bar{q}(s)$  – function describing the relationship between flux and temperature over time.

So we will express the solution to the problem in the formula:

$$\bar{\theta}_k(z, t) = L^{-1} \left[ \bar{\theta}_k(z, s) \right] = \int_0^t \theta_{k0}(z, \tau) q_s(t - \tau) d\tau
 \tag{4.2a}$$

where

$$\theta_{k0}(z, t) = L^{-1} \left[ \bar{\theta}_k(z, s) \Big|_{\bar{q}_s=1} \right]
 \tag{4.2b}$$

As it can be seen, the impedance match between layers 1 and 2 and between layer 3 and the subgrade reduce temperatures in all the pavement courses and also in the subgrade, i.e. in the whole pavement. This will be directly demonstrated by numerical calculations in the further part of this article.

## 5. Examples of numerical analysis for road and airfield pavements using the proposed heat conduction problem solution

The numerical calculations are carried out for daily variations of ambient temperature and solar heat flux for steady-state ( $q_z(t) = q_{z0}e^{i\omega t}$ ) heat flow conditions using the following formula:

$$\begin{aligned}
 (5.1) \quad \theta_k(z, t) &= \operatorname{Re} \int_0^t \theta_{k0}(z, \tau) e^{i\omega(t-\tau)} d\tau = \operatorname{Re} \int_0^t \theta_{k0}(z, \tau) e^{i\omega t} e^{-i\omega\tau} d\tau \\
 &= \operatorname{Re} \left( e^{i\omega t} \int_0^t \theta_{k0}(z, \tau) e^{-i\omega\tau} d\tau \right) \\
 &= \operatorname{Re} \left\{ e^{i\omega t} \left[ \int_0^\infty \theta_{k0}(z, \tau) e^{-i\omega\tau} d\tau - \int_t^\infty \theta_{k0}(z, \tau) e^{-i\omega\tau} d\tau \right] \right\}
 \end{aligned}$$

The steady state solution is given by the following formula for  $t \rightarrow \infty$ :

$$(5.2) \quad \theta_k(z, t) = \operatorname{Re} \left( e^{i\omega t} \int_0^\infty \theta_{k0}(z, \tau) e^{-i\omega\tau} d\tau \right) = \operatorname{Re} \left( e^{i\omega t} \bar{\theta}_{k0}(z, s) \Big|_{s=i\omega} \right)$$

where:  $\bar{\theta}_{k0}(z, s)$  it is expressed as a formula (4.1) for  $\bar{q}(s) = 1$ .

Are described with equations (3.1) for:  $k = 1, 2, 3, p$ ,  $\omega = \frac{2\pi}{T}$ ;  $T$  – length of day in [sec]. The above patterns apply to the classic heat model.

In the case of a heat propagation wave model, the given patterns take the following form:

$$\begin{aligned}
 (5.3) \quad \theta_k(z, t) &= \operatorname{Re} \left( e^{i\omega(t-\frac{z}{c})} \bar{\theta}_{k0}(z, s) \Big|_{s=i\omega} \right), \quad \text{if } -t \geq \frac{z}{c} \\
 &\text{or} \\
 \theta_k(z, t) &= 0, \quad \text{if } -t < \frac{z}{c}
 \end{aligned}$$

Numerical procedure for finding the real part of the complex function expressed by appropriate Laplace transforms, as per the following equations, was used directly in the

temperature distribution calculations.

$$\theta_k(z, t) = \frac{1}{2} \left( e^{i\omega t} \bar{\theta}_{k0}(z, s) \Big|_{s=i\omega} + e^{-i\omega t} \bar{\theta}_{k0}(z, s) \Big|_{s=-i\omega} \right)$$

The nomographs relating to homogenization, which we used in these calculations, come from [24] where they are given in numerical version.

Two example pavements, one designed for roads and the other for airfields, are used in the examples below. The course thicknesses differ much between the two configurations and the detailed physical properties are presented in Table 1.

Table 1. Physical properties of the materials used for the courses of the example road and airfield pavements

Application	Layer	Thickness [m]	Mass bulk density [kg/m <sup>3</sup> ]	Specific heat [J/(kg·°C)]	Conductivity coefficient [W/(m·°C)]*
Roads	Wearing course	0.04	2,200	1,000	2.0
	Binder course	0.08	2,400	900	2.2
	Base course	0.15	2,400	1,200	2.4
	Subgrade	—	2,000	1,100	2.0
Airfields	Wearing course	0.08	2,200	1,000	2.0
	Binder course	0.12	2,400	900	2.2
	Base course	0.25	2,400	1,200	2.4
	Subgrade	—	2,000	1,100	2.0

\* [25].

Moreover, the following assumptions have been made:

- $\kappa = 12$  [W/(m<sup>2</sup> · °C)] for the wearing course (heat conductivity at the ambient air/wearing course interface), takes into account: windspeed, humidity, color,
- $q_0 = 200$  [W/m<sup>2</sup>] heat flux amplitude,
- $T_A = 20^\circ\text{C}$  temperature amplitude.

### 5.1. Comparison of the wave and classical model of heat propagation in the 3-layer pavement system

The classical solution to the heat conduction problem (Fourier model) concerns a parabolic equation described by a single diffusion parameter:  $a^2 = \frac{k}{\rho c}$ .

In this description thermal disturbances propagate at an infinite speed (contrary to what is postulated by physics). The heat transfer solution in our description is based on the Pipkina-Gurtina [23] wave model of heat propagation in which thermal disturbances

propagate at a finite speed:

$$C_T = \sqrt{\frac{a(0)}{\rho C v}}$$

where  $a(t)$  – relaxation function.

Numerical calculations were made for Maxwell type model:

$$a(t) = a_0 \frac{1}{t_0} e^{-\frac{t}{t_0}} \quad \text{or} \quad \bar{a}(s) = a_0 \frac{1}{s t_0 + 1}$$

where:  $a_0$  – conductivity coefficient,  $t_0$  – thermal relaxation time [26].

The difference between the wave propagation of heat and the classical description is particularly significant at the thermal wavefront (particularly evident with pulse type of heat flux action). The situation with the visible forehead of the wavefront thermal is shown in the Figs. 3a, 3b.

The following examples show that in steady-state heat transfer conditions (the thermal wavefront located away from the source), the temperature distributions are similar in these two models.

As it can be seen from Figs. 4, 5, in steady-state conditions ( $t \rightarrow \infty$ ) similar results are obtained with the two models (thermal wave model and the classical one) and the differences are insignificant for the temperature distribution computations. A characteristic feature of the thermal wave model is the wavefront which plays a major role, especially in the pulse thermal load problems.

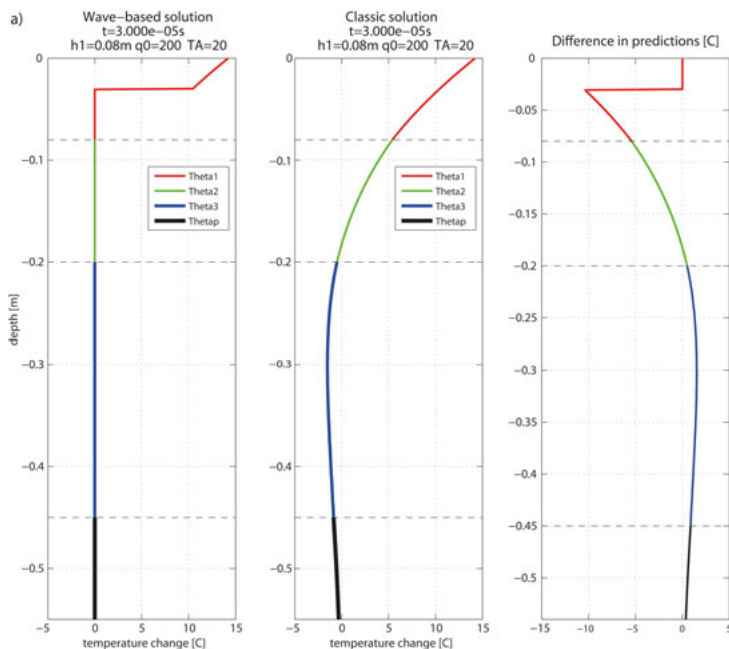


Fig. 3a) Road pavement  $t = 3.000e - 05$  s

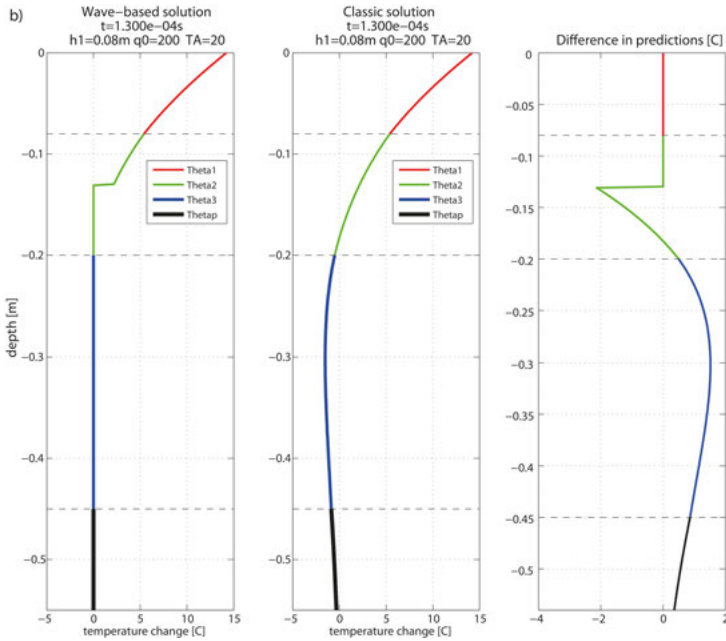


Fig. 3. Comparison of the thermal wave (with propagation thermal wave front) and the classical of heat conduction: a) road pavement  $t = 3.000e - 05$  s, b) road pavement in the time  $t = 1.300e - 04$  s

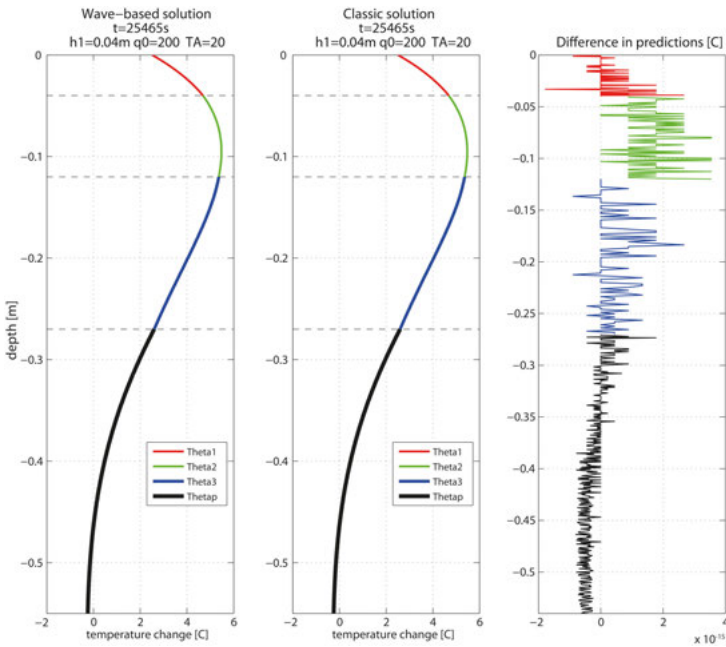


Fig. 4. Comparison of the thermal wave and the classical solution of heat conduction and their relative difference for a road pavement (temperature profile as a function of depth at a specific time  $t$ )

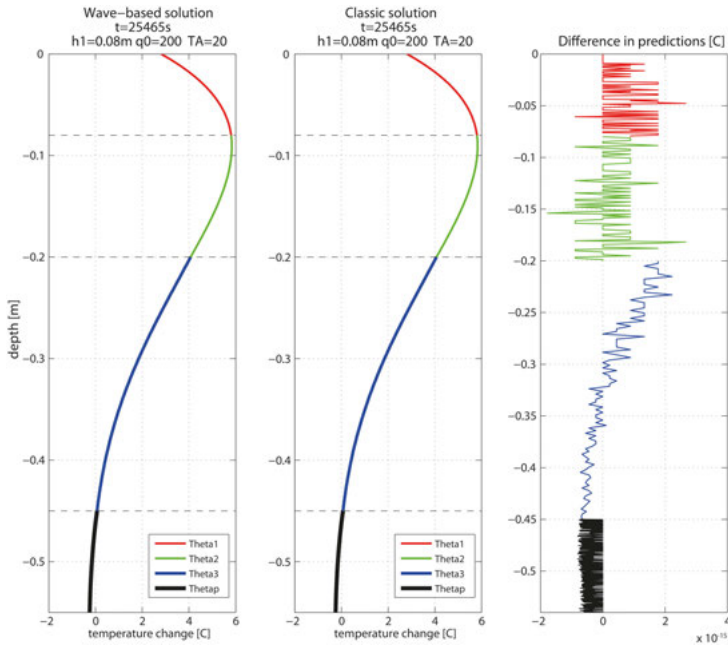


Fig. 5. Comparison of the thermal wave and the classical solution of heat conduction and their relative difference for an airfield pavement (temperature profile as a function of depth at a specific time  $t$ )

## 5.2. Comparison of classical heat conduction solution for the 3-layer and homogenized pavement systems

The 3-layer pavement system has been compared with its homogenized equivalent using the thermal parameters given in Table 1 below. The corresponding thermal parameters of the homogenized equivalent structure are given in Table 2. The temperature profile in the pavement is presented for a specific time and the relative differences between the 3-layer and the homogenized cases are given the same as above.

Table 2. Properties of homogenized systems of road and airfield pavements

Homogenized system	Thickness [m]	Bulk density [kg/m <sup>3</sup> ]	Specific heat [J/(kg·°C)]	Conductivity coefficient [W/(m·°C)]
Road pavement	0.27006	2370.0	1,080.1	2.2715
Airfield pavement	0.45012	2363.0	1,082.3	2.2646

Comparison of the solutions obtained with classical and homogenized road and airfield pavement models (temperature profile as a function of depth at a specific time  $t$  and relative differences between the solutions) are show in the Figs. 6, 7.

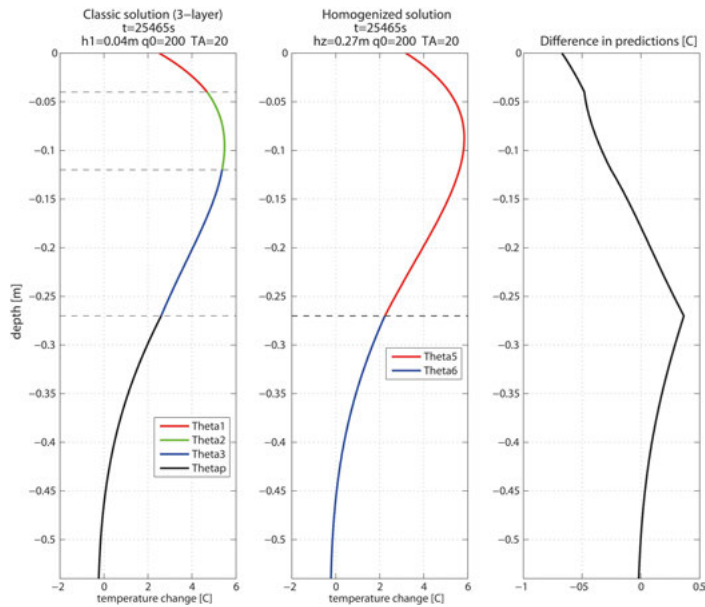


Fig. 6. Comparison of the solutions obtained with classical and homogenized road pavement models (temperature profile as a function of depth at a specific time  $t$  and relative differences between the solutions)

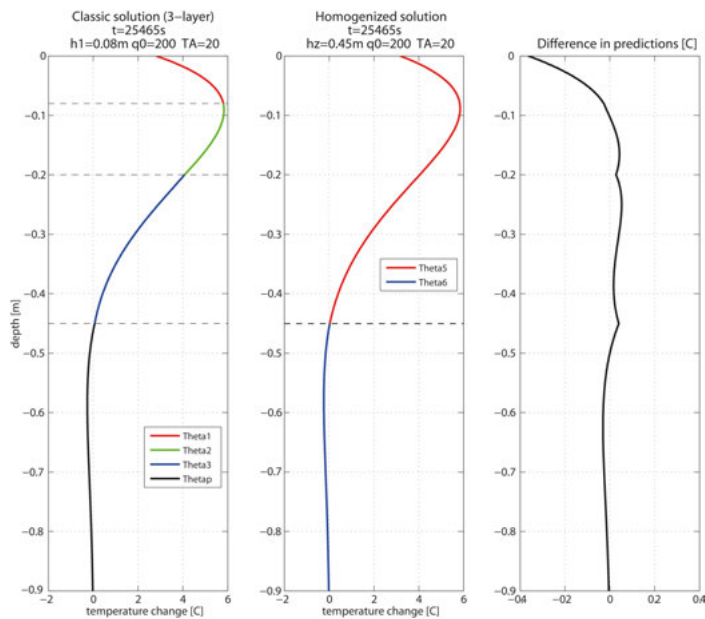


Fig. 7. Comparison of solutions obtained with classical and homogenized airfields pavement models (temperature profile as a function of depth at a specific time  $t$  and relative differences between the solutions)

Comparing the results obtained for the layered and homogenized models we observe good consistency between the temperature distributions. The temperature differences result primarily from the methods of calculating the average values of the thermal quantities from the constants of leptokurtic distribution given in [24] which consider primarily the effect of thickness of a given layer assuming uniform temperature distribution in it. This problem will be solved by modifying the layered pavement system homogenization method.

### 5.3. Demonstration of the effect of thermal compatibility considering the classical heat conduction solution for the 3-layer pavement system

Assuming the real change of the thermal properties of the pavement courses (for example  $r = \sqrt{\frac{\rho_{i+1}c_{i+1}a_{i+1}}{\rho_i c_i a_i}} = 5$  or  $1/5$ ), we obtain the refraction coefficient in the range of  $-0.6$  to  $0.6$ . This would give 25-fold change of the thermal impedances of the adjacent courses which is impracticable in production of road paving materials and thus  $|w| < 0.5$  is adopted in practice.

The thermal impedance of the pavement course materials is calculated with  $i = \sqrt{\rho c a}$ , where:  $\rho$  – mass density of the material,  $c$  – specific heat (representing the thermal storage capacity of the material),  $a$  – thermal conductivity coefficient (representing the thermal conductivity of the material).

A change to any of these parameters will change the thermal impedance of the material and, as a consequence, also the thermal compatibility of the pavement courses. This implies a direct change to the maximum values and temperature distributions in the respective pavement courses.

The functional and structural performance and the pavement life cycle are extended as a result.

The following examples demonstrate the effect of thermal compatibility of pavement courses for the 3-layer system (i.e. the thinner of the previously given examples) with the use of the classical heat propagation solution. The layer parameters and external conditions have been assumed similarly to the previous examples. The refraction coefficients at the interfaces between the layers are consistent with equation (3.5).

It must be noted that the effect of thermal compatibility can be expressed by different resulting parameters related to the obtained time-space field of temperature.

The following examples assume the maximum temperature of the wearing course obtained at any depth and any time in the time-span of the analysis.

Below, as the first in the sequence is a graph presenting the relationship between the maximum temperature in the wearing course as a function of all the three thermal compatibility coefficients (Fig. 8). Next there are three sets of charts (Fig. 9, Fig. 10, Fig. 11) where in each set one coefficient assumes example values of  $-0.99$ ,  $0$ ,  $0.57$  and  $0.99$ .

The top layer (wearing course) is the most sensitive, which sensitivity is expressed by the value of  $T_{\max}$ , to the changes of the refraction coefficients  $w_{3p}$  and  $w_{23}$ . The

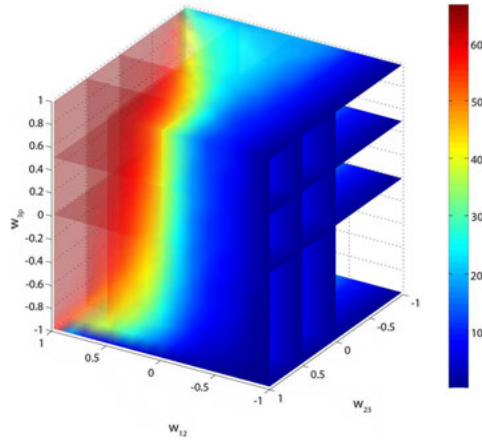


Fig. 8. Illustrative chart of the relationships of the temperature in the first course and the three thermal compatibility coefficients ( $w_{12}$ ,  $w_{23}$ ,  $w_{3p}$ ) determined for the three respective layers of pavement

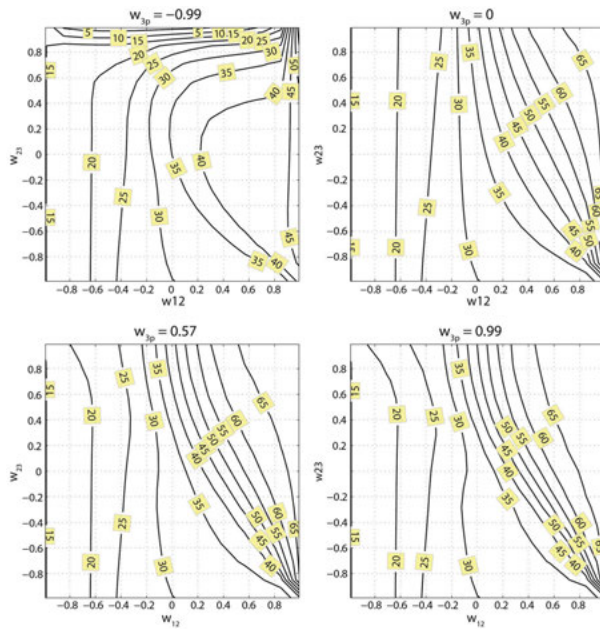


Fig. 9. Graphs showing the effect of  $w_{12}$  and  $w_{23}$  on the maximum temperature in the wearing course for the pre-determined example values of  $w_{3p}$  (-0.99, 0, 0.57 and 0.99)

highest temperature in the top layer, accompanied by small effect the remaining refraction coefficient on the temperature, was obtained with  $w_{12}$  tending to 1.

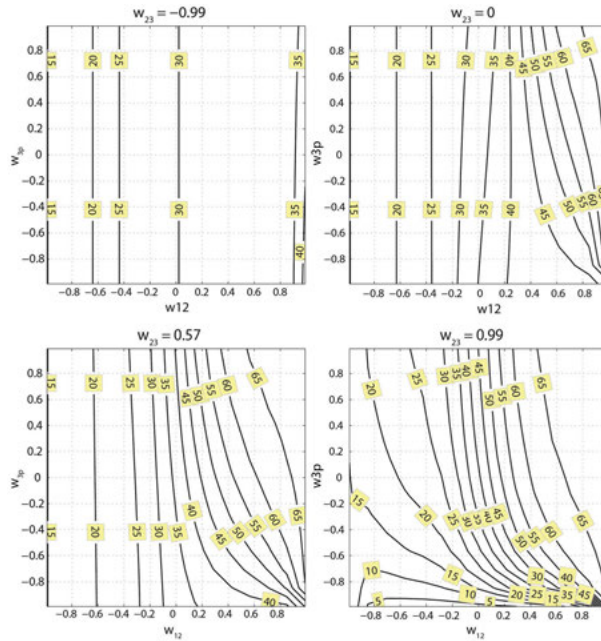


Fig. 10. Graphs showing the effect of  $w_{12}$  and  $w_3$  on the maximum temperature in the wearing course for the pre-determined example values of  $w_{23}$  (-0.99, 0, 0.57 and 0.99)

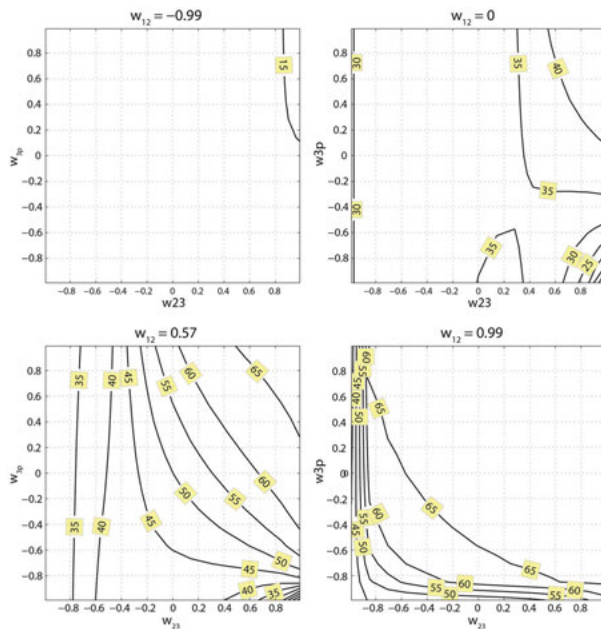


Fig. 11. Graphs showing the effect of  $w_{23}$  and  $w_{3p}$  on the maximum temperature in the wearing course for the pre-determined example values of  $w_{12}$  (-0.99, 0, 0.57 and 0.99)

#### 5.4. Demonstration of the effect of thermal compatibility considering the classical heat conduction solution for the 1-layer pavement system (pavement + subgrade)

The example presented above considers a 3-layer pavement system with three thermal compatibility coefficients. A similar analysis can be performed for a single-layer pavement system (one layer resting on the subgrade). Figure 12 presents the combined effect of the layer thickness and the thermal compatibility coefficient on the maximum temperature in the layer. The values of parameters are taken according to Table 2. It can easily be seen that the thermal compatibility effect (i.e. sensitivity to the value of coefficient  $w$ ) is considerable and incomparably greater for thinner structures. In the case of thinner structures the maximum temperature in the layer can vary more than six times depending on the thermal compatibility coefficient, leading, as a result to a very much different behavior of such road pavements.

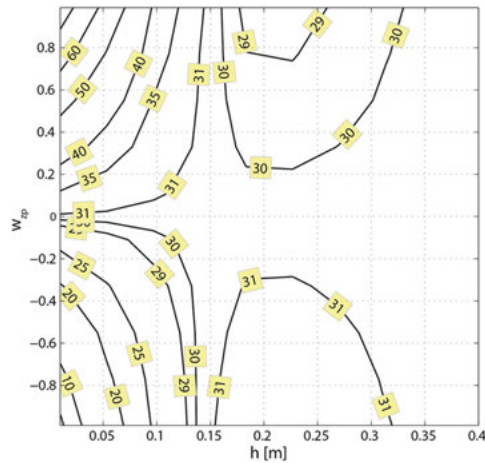


Fig. 12. Combined effect of the layer thickness and the thermal compatibility coefficient between the layer and subgrade on the maximum temperature in the layer

#### 5.5. Demonstration of the effect of thermal compatibility considering the classical heat conduction solution for the 3-layer road and airfield pavement systems

The following example investigates the effect of the layer thicknesses on the maximum temperature in the wearing course. The calculations have been carried out separately for the road and airfield pavements, as per Table 1. The results are illustrated in the graphs: one for the road and the other for the airfield pavement for the pre-defined values of  $w_{23}$  and  $w_{3p}$  adopted following analysis of results from the previous examples. The parameters are taken according to Table 1, except that in order to check the sensitivity of the proposed solution to the wearing course thickness the calculations were repeated for different values of  $h_1$  in

order to obtain, for the two pavements, the influence lines with the same values of  $h_1/h_2$  in the range of 0.125–1. As it can be seen in Fig. 13 and in Fig. 14 the influence lines follow a similar path for the two pavement systems. The thermal compatibility coefficient was found to be of primary importance to the large (i.e. along the  $h_1/h_2 = 0.125$  line) disproportion of the layer thicknesses. A considerably smaller effect of this thermal compatibility coefficient was obtained for pavements in which the wearing course has the same thickness as the binder course. Moreover, it is attributed solely to differences in the thermal parameters.

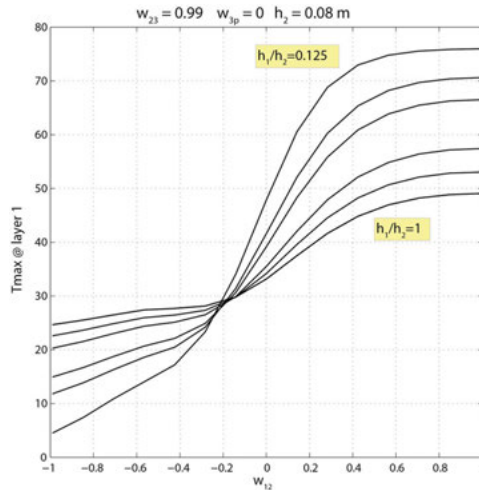


Fig. 13. Curves showing the effect of the wearing course thickness and the thermal compatibility coefficient  $w_{12}$  on the maximum temperature in the road pavement ( $h_2 = 0.08$  m)

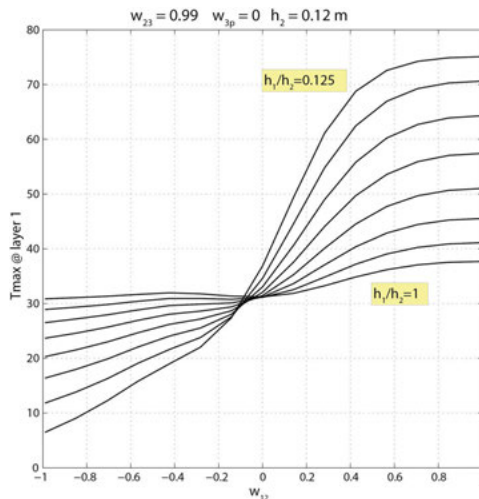


Fig. 14. Curves showing the effect of the wearing course thickness and the thermal compatibility coefficient  $w_{12}$  on the maximum temperature in the airfield pavement ( $h_2 = 0.12$  m)

## 6. Summing up

This article presents a new analytical solution to the problem of heat transfer and vertical distribution of temperature in multi-layered road and airfield pavements. This new solution provides a more accurate representation of the actual structural systems of existing road and airfield pavements. A unique thermal wave propagation model is proposed as part of this solution, considering generalized boundary conditions. Physical refraction at the interfaces between the pavement courses is described analytically. The predictions obtained with the thermal wave model of heat propagation are compared with the classical model values. The solution to the problem of heat conduction and refraction in an multi-layered pavement was presented in an innovative manner using a description of thermal wave conduction through a multi-layered system, comprising three pavement courses and the soil subgrade, considering refraction and heat exchange effects inside the pavement.

A detailed analysis was carried out for the conduction of heat through a multi-layered pavement system comprising the following courses:

- surfacing (comprising a sequence of asphalt layers for example),
- base course,
- soil subgrade.

Moreover, the solutions were obtained, and the consistency of results was checked for the multi-layered model and its homogenized equivalent according to the solution presented in [24]. The results obtained for the multi-layered and homogenized pavement systems were compared. The problem was solved with the classical and the thermal wave heat propagation models and a high degree of consistency between the results obtained with these two models was found.

A numerical analysis was carried out for various multi-layer pavement systems and the results were found to be highly consistent with the formulated hypotheses.

The research outputs provide a new tool for evaluating the existing road pavements in terms of thermal actions and enable optimizing the design aspects relating the new pavement courses in order to mitigate the undesired thermal and climatic impacts. The results of this research provide the grounds for the pavement production investigations aimed at minimizing the external thermal and climatic effects on a multi-layer pavement.

The research demonstrated a combined effect of external actions (flux of thermal radiation) and Newtonian heat exchange with the thermal properties of the paving materials on the vertical distribution of temperature and heat conduction in a multi-layer pavement system. In addition to the ambient air temperature also solar radiation is to be considered a relevant climatic factor which acting directly on the top surface, increases the temperatures and creates an additional temperature gradient in a multi-layer pavement.

Moreover, the research demonstrates that the vertical temperature distribution in multi-layer pavements depends, to a large extent, on the geometric configuration of the pavement courses, their thermal properties, expressed by thermal impedances and the heat exchange coefficient at the boundary with external medium, which depends on the top surface color, humidity wind speed and material a going [27, 28]. The results obtained in the research are illustrated by example distributions of temperature, heat conduction and refraction in

different pavement systems. The quantitative effect of thermal impedances of the pavement materials  $i = \sqrt{\rho c a}$ , i.e. density, specific heat and thermal conductivity on the performance characteristic of road and airfield pavements is also demonstrated. It is presented in a simplified way and from a different angle in Fig. 15. As it can be seen, a combination of coefficients  $w_{12}$  and  $w_{23}$  (Fig. 15c) had the greatest effect on the maximum temperature in the wearing course, with considerably smaller effect of coefficient  $w_{3p}$ .

The maximum temperature value in layers depends significantly on the thermal compatibility value. Materials used for paving construction should be selected and tested not only in terms of mechanical but also thermal parameters.

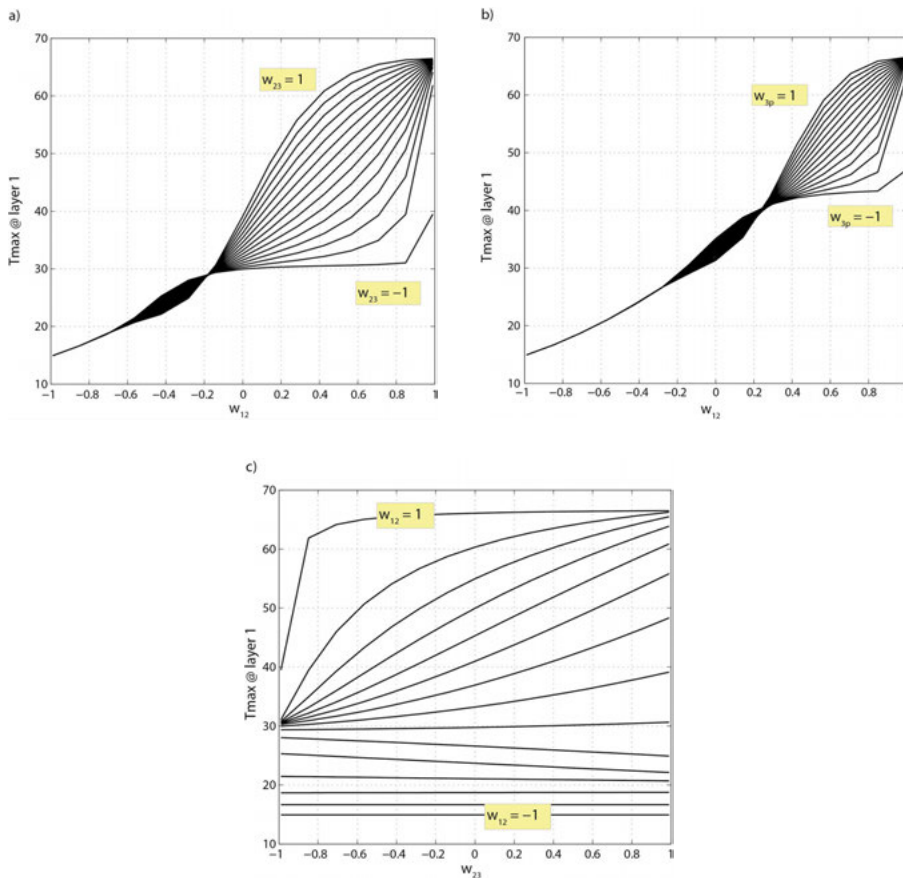


Fig. 15. Graphs showing the effect of the thermal compatibility coefficients on the maximum temperature in the road pavement: a) with  $w_{3p} = 0$ , b) with  $w_{23} = 0$ , c) with  $w_{12} = 0$

The maximum temperature value in layers depends significantly on the thermal compatibility value. Materials used for paving construction should be selected and tested not only in terms of mechanical but also thermal parameters.

Finally, this research provides guidance for actions to be undertaken in order to reduce the effect of changing climatic conditions on the operation of multi-layer flexible road and airfield pavements [6].

## References

- [1] P. Moon, D.E. Spencer, *Field theory for engineers*. Princeton USA: Van Nostrand Company, 1961.
- [2] H.F. Southgate, *An evaluation of temperature distribution of asphalt pavements and its relationship to pavement deflection*, MSCE Thesis, University of Kentucky, Lexington, Kentucky, 1968, DOI: [10.13023/KTC.RR.1968.253](https://doi.org/10.13023/KTC.RR.1968.253).
- [3] R.N. Stubstad, S. Baltzer, E.O. Lukanen, H.J. Ertman-Larsen, *Prediction of AC mat temperature for routine load/deflection measurements*, in Proceedings 4th International Conference on Bearing Capacity of Road and Airfields, July 17–21, 1994, Minnesota, 1994.
- [4] E.O. Lukanen, R.N. Stubstad, R. Briggs, *Temperature prediction and adjustment factors for asphalt pavement*, Report No FHWA-RD-98-085. McLean, Virginia: Federal Highway Administration, 2000.
- [5] D. Sybilski, K. Mirski, “Zalecane lepiszcza asfaltowe w warstwach nawierzchni w Polsce z uwzględnieniem warunków klimatycznych i obciążenia ruchem”, (“Recommended asphalt binders in pavement layers in Poland taking into account climatic conditions and traffic loads”), *Prace IBDiM*, 2000, no. 1-2, pp. 103–157 (in Polish).
- [6] D.Y. Park, N. Buch, K. Chatti, “Effective layer temperature prediction model and temperature correction using FWD deflections”, *Transportation Research Record: Journal of the Transportation Research*, 2001, vol. 1764, no. 1, DOI: [10.3141/1764-11](https://doi.org/10.3141/1764-11).
- [7] P. Mieczkowski, “Model fizyczny obliczania temperatury górnej warstwy nawierzchni asfaltowej”, (“Physical model for calculating the temperature of the upper layer of asphalt pavement”), *Drogownictwo*, 2001, nr 8, pp. 230–235.
- [8] A. Hermansson, “Simulation of asphalt concrete (AC) pavement temperatures for use with FWD”, *Road Materials and Pavement Design*, 2002, vol. 3, no. 3, pp. 281–297, DOI: [10.1080/14680629.2002.9689926](https://doi.org/10.1080/14680629.2002.9689926).
- [9] L. Rafalski, “Podłoże nawierzchni drogowej”, *Inżynieria Morska i Geotechnika*, 2009, nr 3, pp. 190–193.
- [10] M. Wistuba, “Determining design temperatures for asphalt pavements”, *Road Materials and Pavement Design*, 2003, vol. 4, no. 3, pp. 341–349, DOI: [10.1080/14680629.2003.9689953](https://doi.org/10.1080/14680629.2003.9689953).
- [11] M. Wistuba, R. Blab, J. Litzka, *Oberbauverstarkung von asphaltstrassen. Methodenüberblick und Ableitung von Klimadaten für die analytische Bemessung*. Wien, 2004.
- [12] J. Górszczyk, W. Grzybowska, “Analizy termiczne asfaltowej nawierzchni drogowej z wykorzystaniem MES” (“The use of FEM for thermal analyses of the asphalt pavement”), *Roads and Bridges – Drogi i Mosty*, 2011, vol. 10, no. 4, pp. 5–30.
- [13] D. Wang, “Analytical Approach to Predicting Temperature Fields in Multi-layer Pavement Systems”, *Journal of Engineering Mechanics*, 2009, vol. 135, no. 4, pp. 334–344, DOI: [10.1061/\(ASCE\)0733-9399\(2009\)135:4\(334\)](https://doi.org/10.1061/(ASCE)0733-9399(2009)135:4(334)).
- [14] D. Wang, J.R. Roesler, “One-dimensional temperature profile prediction in multi-layer rigid pavement systems using a separation of variables method”, *International Journal of Pavement Engineering*, 2014, vol. 15, no. 5, pp. 373–382, DOI: [10.1080/10298436.2011.653358](https://doi.org/10.1080/10298436.2011.653358).
- [15] M.R. Hall, et al., “Influence of the Thermophysical Properties of Pavement, Materials on the Evolution of Temperature Depth Profiles in Different Climatic Regions”, *Journal of Materials Civil Engineering*, 2012, vol. 24, no. 1, pp. 32–47, DOI: [10.1061/\(ASCE\)MT.1943-5533.0000357](https://doi.org/10.1061/(ASCE)MT.1943-5533.0000357).
- [16] P. Bryant, E. Denneman, *Improved Design Procedures for Asphalt Pavements: Pavement Temperature and Load Frequency Estimation. Austroads Technical Reports APT248-13*. September 2013, Sydney, Australia 2013.
- [17] *Guide for Mechanistic Empirical Design – Final Report, Part Two. Design Inputs Chapter Environmental Effects*, NCHRP, March 2004.

- [18] S. Parison, M. Hendel, A. Grados, K. Jurski, L. Royon, "A radiative technique for measuring the thermal properties of road and urban materials", *Road Materials and Pavement Design*, 2021, vol. 22, no. 5, pp. 1078–1092, DOI: [10.1080/14680629.2019.1661869](https://doi.org/10.1080/14680629.2019.1661869).
- [19] A. Toktorbai Uulu, H. Katsuchi, H. Kim, H. Yamada, Y. Ijima, "Study on thermal parameters of asphalt concrete for countermeasures against high surface temperature of pavement in tunnel", *Road Materials and Pavement Design*, 2021, vol. 22, no. 4, pp. 954–968, DOI: [10.1080/14680629.2019.1651757](https://doi.org/10.1080/14680629.2019.1651757).
- [20] T. Sok, Y.K. Kim, S.W. Lee, "Numerical evaluation of built in temperature distribution effects on stress development in concrete pavements", *Road Materials and Pavement Design*, 2021, vol. 22, no. 4, pp. 871–893, DOI: [10.1080/14680629.2019.1691044](https://doi.org/10.1080/14680629.2019.1691044).
- [21] M. Graczyk, "Nośność konstrukcji nawierzchni wielowarstwowych w krajowych warunkach klimatycznych", ("Bearing capacity of multi-layer pavement structures in national climatic conditions"), in *Studia i Materiały*, z. 63. Warszawa: IBDiM, 2010.
- [22] M. Graczyk, J. Rafa, L. Rafalski, A. Zofka, "New Analytical Solution of Flow and Heat Refraction Problem in Multilayer Pavement", *Roads and Bridges – Drogi i Mosty*, 2014, vol. 13, no. 1, pp. 33–48; DOI: [10.7409/rabdimm.014.003](https://doi.org/10.7409/rabdimm.014.003).
- [23] M.E. Gurtin, A.C. Pipkin, "A general theory of heat conduction with finite wave speeds", *Archive for Rational Mechanics and Analysis*, 1968, vol. 31, pp. 113–126, DOI: [10.1007/BF00281373](https://doi.org/10.1007/BF00281373).
- [24] M. Graczyk, J. Rafa, A. Zofka, "Pavement modelling using mechanical and thermal homogenization of layered systems", *Roads and Bridges – Drogi i Mosty*, 2018, vol. 17, no. 2, pp. 141–157, DOI: [10.7409/rabdimm.018.009](https://doi.org/10.7409/rabdimm.018.009).
- [25] R. Petkova-Slipets, P. Zlateva, "Thermal Properties of a New Pavement Material for Using Road Construction", *Civil and Environmental Engineering*, 2018, vol. 14, no. 2, pp. 99–104, DOI: [10.2478/cee-2018-0013](https://doi.org/10.2478/cee-2018-0013).
- [26] J. Gawinecki, A. Gawinecka, J. Łazuka, J. Rafa, "Mathematical and physical aspects of the initial value problem for a nonlocal model of heat propagation with finite speed", *Applicationes Mathematicae*, 2013, vol. 40, pp. 31–61, DOI: [10.4064/am40-1-3](https://doi.org/10.4064/am40-1-3).
- [27] X. Li, A. Zofka, M. Morasteanu, T. Clyne, "Evaluation of Field Aying Effects on Asphalt Blunder Properties", *Road Materials and Pavement Design*, 2006, vol. 7, sup. 1, pp. 57–73, DOI: [10.1080/14680629.2006.9690058](https://doi.org/10.1080/14680629.2006.9690058).
- [28] R. Nagórski, *Mechanika nawierzchni drogowych w zarysie*. Warszawa: Wydawnictwo Naukowe PWN, 2014.

## Analityczne rozwiązanie modelu falowego propagacji ciepła w konstrukcji nawierzchni

**Słowa kluczowe:** nawierzchnia wielowarstwowa, klasyczny i falowy model propagacji ciepła, układ zastępczy (zhomogenizowany), współczynnik refrakcji, kompatybilność termiczna

### Streszczenie:

Nawierzchnie w układzie geometrycznym i fizycznym są konstrukcjami warstwowymi. Najczęściej w nawierzchniach podatnych występuje pakiet asfaltowy w układzie warstwa ścierna, warstwa wiążąca i podbudowa. Dotychczas nie ma ścisłego rozwiązania analitycznego takiego układu warstwowego w odniesieniu do rozkładu temperatury z uwzględnieniem charakterystyk cieplnych każdej z warstw oraz z zachowaniem praw fizycznych falowego przepływu ciepła. W konsekwencji, nie ma możliwości oceny wpływu cech termicznych poszczególnych warstw na rozkład temperatury w całym pakiecie asfaltowym. W nawierzchni wielowarstwowej istotną rolę odgrywają także zjawiska zachodzące na granicach kolejnych warstw, które mają wpływ na trwałość całej konstrukcji jezdni.

W pracy przedstawiono nowe rozwiązanie analityczne zagadnienia przepływu i refrakcji ciepła w nawierzchni warstwowej. Na podstawie uzyskanego rozwiązania zbadano i określono wpływ falowego charakteru propagacji ciepła na rozkład temperatur uwzględniając jednocześnie warstwowość konstrukcji nawierzchni: podłoże gruntowe – podbudowa – warstwa jezdna. Dokonano także porównania rozwiązania klasycznego przepływu ciepła z rozwiązaniem falowym w układzie warstwowym nawierzchni oraz porównania rozkładu temperatury w nawierzchni w układzie warstwowym z układem zhomogenizowanym.

Rozwiązanie problemu przewodnictwa ciepła w układzie warstwowym wykazało znaczący wpływ wprowadzonych przez autorów współczynników dopasowania termicznego oraz refrakcji termicznej warstw na rozkład temperatur w konstrukcji nawierzchni warstwowej. Wynikiem pracy jest wyznaczenie rozkładu temperatury w nawierzchni oraz wskazanie kierunków działań zmniejszających wpływ zmiennych warunków klimatycznych na eksploatację wielowarstwowych podatnych nawierzchni drogowych i lotniskowych. Uzyskane rezultaty są także nowym elementem wzbogacającym możliwości oceny oddziaływania termicznego na rzeczywistą konstrukcję nawierzchni.

Received: 16.07.2021, Revised: 14.09.2021